

**CROSS FLOW DRAG ON A SEGMENTED MODEL**

**BY**

**Ing. W. Beukelman**

**Report 831-P**

**Ship Hydromechanics Laboratory  
Delft University of Technology  
The Netherlands  
October 1989**

## CROSS FLOW DRAG ON A SEGMENTED MODEL

by  
ing. W. Beukelman\*

Ship Hydromechanics Laboratory, Delft University of Technology,  
Mekelweg 2, 2628 CD Delft, The Netherlands

### ABSTRACT

Drift forces have been measured on a seven-segmented ship model for drift angles up to 20 degrees at different forward speeds. These experiments have been carried out for three different draughts and also at 3.4 degree bow and stern trim for the design draught. For each section the linear and non-linear part of the drift force have been determined as well as the cross flow drag coefficient to find the longitudinal distribution of the coefficients related to speed and drift angle. Similar relations have also been determined for the whole ship model. It appeared that for even keel and bow trim the forward sections contribute the most dominant part of the drift forces while for trim by stern higher drift forces with a more equal distribution along the ship length are produced. Calculated values based on strip theory, also taking into account the influence of the bottom have been compared with measured values derived from the linear part of the drift forces and showed rather good agreement for the forward part of the model. A practical calculation method for determining the linear drift force coefficient in combination with a cross flow drag estimated from experiments, provides a good approximation of the total drift force coefficient.

### NOMENCLATURE

$A_{wl}$	waterplane area
B	beam
$C_B$	blockcoefficient
C	cross flow drag coefficient
$Fn = \frac{U}{\sqrt{gL_{pp}}}$	Froude number
g	acceleration due to gravity
h	waterdepth
$L_{pp}$	length between perpendiculars
$L_{wl}, L$	length on the waterline
$l_s$	length of section
m	added mass
N	drift force moment; potential damping coefficient
T	draught of model
U	forward speed
v	transverse speed (positive to starboard)

Y	drift force
$\alpha$	trim angle (positive for bow down)
$\beta$	drift angle
$\rho$	density of water
V	volume of displacement of model

### Subscripts

D	drag
ln	linear
nl	non-linear
v	derivatives $\partial/\partial v$

### Superscripts

*	asterix for value of segment
'	indication for sectional value; indication for non-dimensional coefficient

### INTRODUCTION

As announced by dr. J.P. Hooft of MARIN at the 18th ITTC [1] the Ship Hydromechanics Laboratory of the Delft University of Technology has on his instigation carried out a series of tests with a seven-segmented ship model to determine the distribution of the drift force and the cross flow drag over the length of the model. Up to now only a few experiments have been reported with segmented models for the derivation of the local cross flow drag coefficient; see [2] and [3]. Recently Matsumoto and Suemitsu reported in [4] similar experiments with a ten-segmented ship model. They showed an almost identical distribution of the cross flow drag coefficient over the ship's length as found in this study. Included here are also the results of the static drift angle experiments carried out with the same above mentioned seven-segmented model in different waterdepths as reported in [5] and referred to in the proceedings of the 17th ITTC [6]. These experiments formed part of an investigation to determine the longitudinal distribution of low frequency hydrodynamic derivatives for lateral motions in shallow water. Another experimental study on manoeuvring hydrodynamic forces in shallow water was carried out by Hirano et al.

\* Associate Professor

[7]. Force measurement tests by means of a PMM were performed with use of three kinds of ship models at various waterdepths. The results showed the same tendency related to the hydrodynamic derivatives of the hull as found in [5, 6] for shallow water.

Hydrodynamic derivatives on ship manoeuvring in trimmed condition have also been investigated by Inoue et al. as presented in [8] and [9]. Trim by stern delivered in their studies almost linear increase of lateral forces with the trim. Also Gerritsma found a significant increase of the drift force for trim by stern [10]. To gain more insight in the dependency of the drift force to the longitudinal position, drift angle, forward speed, model trim and sinkage, it was decided to carry out static drift experiments with a seven-segmented model varying the mentioned parameters. This total drift force was for each section divided into a linear and non-linear component. In this way the longitudinal distribution could be estimated for both the total and the linear part of the drift force. From the non-linear part of the drift force the cross flow drag coefficient has been derived as well as the longitudinal distribution of this coefficient. More detailed information about the experiments only has been presented in [11].

Strip theory calculations have been performed for deep and shallow water. For the last mentioned case use has been made of Keil's method as presented in [12]. The influence of the bottom on the drift forces should be taken into account earlier than supposed up to now. All calculations are based on the assumption of an ideal fluid, thus neglecting the effects of viscosity. A comparison of the experimental values related to the linear part of the drift forces and the calculated values show the influence of viscosity on the distribution of the hydrodynamic derivative in particular aft of the midship section. Because of the separation effects in this region the application of strip methods remains questionable. Nevertheless, for this ship type an attempt has been made to present a rough estimate for the determination of the linear drift coefficient which in combination with an expression for the influence of the cross flow drag based on experiments, delivers a value for the total drift force coefficient.

#### DESCRIPTION OF EXPERIMENTS

Static drift angle experiments have been performed with the well known 2.3 meter model of the Todd Sixty Series.

Table 1

Length between perpendiculars	$L_{pp}$	2.258 m
Length on the waterline	$L_{wl}$	2.296 m
Beam	B	0.322 m
Draught	T	0.129 m
Volume of displacement	V	0.0657 m <sup>3</sup>
Block coefficient	$C_B$	0.70
Waterplane area	$A_{wl}$	0.572 m <sup>2</sup>
LCB forward of L/2		0.011 m
LCF aft of L/2		0.038 m

The model has been tested without rudder and propeller. The same model has been used earlier for analogous tests in deep and shallow water [5, 6]. The model has been divided into seven segments each of which was separately connected to a strong beam by means of a strain gauge dynamometer. These dynamometers measured horizontal forces perpendicular to the longitudinal centerline of the model only.

All sections have for the design condition a length  $l_s = 0.323$  meter except for the last section nr.1 which has a length of  $l_s = 0.360$  meter. The experimental set up as used for the oscillation tests is shown in figure 1. The test conditions considered are summarized in table 2.

Table 2

nr	T m	L m	$\alpha$ deg.	$F_n$	$\beta$ degrees	h/T
1	0.129	2.295	0	0.0675 0.103	$\pm 2, 4, 6, 8, 10$	2.4
2	0.129	2.295	0	0.15 0.20 0.25	$\pm 4, 8, 12, 16, 20$	15
3	0.129	2.233	+3.4 bow down	0.15 0.25	$\pm 4, 8, 12, 16, 20$	15
4	0.129	2.314	-3.4 bow up	0.15 0.25	$\pm 4, 8, 12, 16, 20$	15
5	0.159	2.320	0	0.15 0.25	$\pm 4, 8, 12, 16, 20$	12
6	0.099	2.216	0	0.15 0.25	$\pm 4, 8, 12, 16, 20$	20

Test condition nr.1 has been considered with former experiments and the results have been reported in [5] and [6]. It has been taken into consideration again to complete the variation of the conditions related to the present study especially with respect to the restricted waterdepth and the lower values of forward speed. At the end of the model, fore and aft, tell tales have been attached to the hull surface in order to establish if and when separation occurred.

#### RESULTS OF EXPERIMENTS

For each section the total drift force  $Y^*$  has been measured from which may be determined the coefficient:

$$Y_v^* = \frac{Y^*}{-U \sin \beta} = \frac{Y^*}{v} \quad (1)$$

in which U - the forward speed and  $v = -U \sin \beta$

The dimensionless coefficient for each segment is expressed as:

$$Y_v^{*'} = \frac{Y_v^*}{0.5 \rho L^2 U} \quad (2)$$

which, upon substitution of (1), becomes

$$Y_v^{*'} = \frac{Y^*}{0.5 \rho L^2 U^2 \sin \beta} \quad (3)$$

This coefficient  $Y_v^{*'}$  has been determined for all conditions on the basis of a positive drift angle being an average value of both the positive and negative drift angle to eliminate asymmetrical hull form influences with respect to the centerline. From these observations for each section the linear and non-linear part of the drift force coefficient have been established in a graphical way which yields:

$$Y_v^{*' } = Y_{vl}^{*' } + Y_{vn1}^{*' } \quad (4)$$

The cross flow drag coefficient for each section is defined as:

$$C_D^* = \frac{Y_{n1}^{*' }}{0.5 \rho L T^* |v|} \quad (5)$$

The coefficients for the whole model as sum of

the sectional values are shown for all conditions considered in figure 2 as  $Y_v'$  for the total drift force, in figure 3 as  $Y_{vln}$  for the linear component of the drift force and in figure 4 as  $C_D$  for the cross flow drag.

The longitudinal distribution of  $Y_v'$ ,  $Y_{vln}$  and  $C_D$  is presented as  $Y_v''$ ,  $Y_{vln}''$  and  $C_D''$  respectively in the figures 5-9 for the denoted conditions. The horizontal drawn line denotes the average measured value of each segment. The coefficients  $Y_v''$ ,  $Y_{vln}''$  and  $C_D''$  are defined by:

$$Y_v'' = \frac{Y_v'}{l_s}, \quad Y_{vln}'' = \frac{Y_{vln}'}{l_s}, \quad C_D'' = \frac{C_D}{l_s}$$

where  $l_s$  = the length of the section under consideration. A possible continuous curve for the coefficients  $Y_v''$ ,  $Y_{vln}''$  and  $C_D''$  has been achieved in the figures 5-9 by taking into account the condition that for each segment the average value should be reproduced.

#### Calculations

For the calculations of  $Y_v''$  use has been made of a two-dimensional multipole approximation following the method of Keil [12] and taking into account the influence of the bottom. After Lewis-transformation the sectional added mass  $m$  and damping  $N$  have been determined for the even keel condition (nr.1 and 2) at the design draught.

For manoeuvring frequencies approaching zero value the influence of the potential damping  $N$  may be neglected. What remains for the damping is the derivative of the sectional added mass in longitudinal direction multiplied with the forward speed. Viscous effects are not taken into account up to now. To show the influence of the bottom

$$Y_v'' = -m' * \frac{1}{0.5\rho L^3} \quad (6)$$

$$\text{and } Y_v'' = -U \frac{dm'}{dx} * \frac{1}{0.5\rho L^2 U}$$

have been calculated for sect.nrs.0-20 in case of the following waterdepth-draught ratio's:

$$h/T = 5000, 77, 15, 5, 2.4, 1.5, 1.15$$

The results are shown in table 3a and b from which it may be clear that the influence of the bottom already starts at  $h/T=15$  and becomes significant at  $h/T=5$ . It should be remarked that integration over the ship's length of

$$Y_v'' = -\frac{dm'}{dx} \frac{1}{0.5\rho L^2}$$

delivers a zero value for

$$Y_v' = \int_{A_{pp}}^{F_{pp}} Y_v'' dx$$

in case there is no sectional area at the end sections. Because of separation phenomena after the midship section it is sometimes proposed to integrate  $Y_v''$  from  $F_{pp}$  to a certain ordinate after midship. In this case the integration has been carried out up to ordinate 8. This choice depends on the experimental curve for  $Y_v''$  which will be discussed later on. Integration from  $F_{pp}$  up to ordinate 8 leads to

$$Y_v'' = -\frac{1}{0.5\rho L^2} \int_{ord.8}^{F_{pp}} \frac{dm'}{dx} dx = -\frac{m'(ord.8)}{0.5\rho L^2} \quad (7)$$

and for the moment of the drift force

$$N_v'' = \int_{ord.8}^{F_{pp}} Y_v' x dx \quad (8)$$

These calculated results,  $Y_v''$  and  $N_v''$ , have been compared in table 4 with the experimental results and the results calculated according to the method of Norrbin [13] and Inoue [14]. For this comparison the same waterdepth-draught ratio's have been taken into consideration as mentioned before. The results of table 4 also show the significance of the bottom influence from  $h/T=5$ . The calculated sectional results  $Y_v''$  are shown in figure 5 for  $F_n = 0.0675, 0.103, 0.15, 0.20$  and  $0.25$  at the considered evenkeel condition. In this figure these results are compared with the linear drift force coefficient  $Y_{vln}''$ , because strip theory calculations as applied above assume linearity of the forces with respect to the drift angle.

#### DISCUSSION OF RESULTS

##### General remarks

It should be emphasised that only forces and no moments on the sections have been measured, so that only an estimation of the longitudinal distribution of these forces may be presented. Especially at the ends of the model it is difficult to give such an estimation. For this reason open ends are presented in the figures showing the longitudinal distribution of the drift forces. It may be expected that the values at the ends should be zero but up to now it is unknown how this zero value will be achieved. Nevertheless an estimated distribution of the drift forces at the ends has been determined to obtain some experimental values for the drift force moment coefficient  $N_v''$ , as presented in table 4, for the shallow water conditions as investigated in [5]. This table 4 clearly demonstrates the influence of water depth on the drift forces and moments. The tell tales attached to the surface of the hull showed also no disturbance at the stern, not even at the highest drift angle and forward speed. In this way it was not possible to establish separation phenomena. Further and more detailed investigations are required in the future.

##### Total model values

The linear drift force coefficient  $Y_{vln}$  for the whole model is almost independent of forward speed. See figure 3. For trim by stern and the largest draught the value of the linear drift force coefficient is considerably higher than for bow trim and smaller draught, as to be expected. The cross flow drag coefficient representing the influence of the non-linear component of the drift force may generally be neglected for drift angles below 4 degrees. See figure 4. Above this drift angle of 4 degrees there is in general a linear increase of the cross flow drag coefficient with the drift angle. For more shallow water ( $h/T=2.4$ ) this coefficient is much lower than for deep water ( $h/T=15$ ) while in general this coefficient increases with speed reduction.

The cross flow drag coefficient shows higher values for bow trim and large draught than for trim by stern and small draught. Related to trim this effect is contrary to that for the linear drift force coefficient. The total drift force coefficient for the whole model is almost independent of forward speed. The linear increase with drift angle is for a great deal due to cross flow. Figure 2 shows that the linear increase of the total drift force coefficient starts at  $\beta = \pm 4$  degrees with the value of the linear drift force coefficient. Experimental analyses of the conditions considered here, resulted in the following expression for the average value of the total drift force coefficient:

$$Y'_v(\beta) = Y'_{vln}(\beta=0-4) + 0.51(\beta-4) \quad (9)$$

$\beta > 4$

in which  $0.51(\beta-4)$  for  $\beta > 4$  represents the influence of the cross flow drag.

#### Longitudinal distribution

For the design draught the distribution over the model length of the linear drift force coefficient  $Y'_{vln}$  shows little dependency on forward speed. See figure 5. Only at sections 5 and 6 some variation with speed is shown mainly because of wave influence due to speed. For bow trim the linear forces of both forward sections increase strongly while a longer positive value over the last part of the model has been shown. The condition trim by stern shows a more equal distribution of higher negative values with in general little speed influence except for section 6 which is probably also due to wave generation at higher speed. For large and small draught respectively the linear force component increases or reduces with draught. Also possible wave influence at the highest speed has been shown at the sections 5 and 6. The calculated distribution of the sectional linear drift force for the even keel condition with  $T = 0.129m$  is also shown in figure 5. For the forward part of the model the agreement between calculated and experimental values is quite reasonable. For the most forward section the average values of calculation and experiment appeared to be almost equal although the depicted distribution curves differ considerably. However, one should keep in mind that the experimental distribution has been estimated from average values. For the aft part of the model the difference between experiment and calculation is significant, especially for  $h/T = 2.4$ . The experimental distribution curve is attaining negative values at the back while the calculated distribution increases to high positive values. This difference might be caused by separation phenomena although this has not been confirmed experimentally with the tell tales. Looking from the back at the experimental distribution of the linear drift force it may be established that somewhere at the aft part a point is situated where there is a balance between negative and positive linear drift forces. This point is estimated to be at section 3 near ordinate 8. If agreement between the calculated and experimental distribution forward of ordinate 8 is accepted, this ordinate may be considered as a point up to which the integration of the calculated linear drift force distribution may be carried out for comparison with experimental values. The results in table 4 show a rather

good agreement between experimental and calculated values except for the lowest waterdepth-draught ratio  $h/T = 1.15$ . The longitudinal distribution of the cross flow drag coefficient shows almost no influence because of drift angle and may in general be neglected for drift angles below 4 degrees as shown in figure 8 and 9. The cross flow may also be neglected for the design draught at both lowest speeds below  $\beta = 6$  degrees and for the three higher speeds below  $\beta = 4$  degrees. Forward speed influence is small for  $Fn = 0.15$ , strong especially at the most forward section for  $Fn = 0.20$  and for  $Fn = 0.25$  particularly important on section 5. For bow trim the values for cross flow are mostly dominant negative for the aft part of the model while at the highest speed strong variations due to wave generation are shown especially over the sections 3, 4 and 5. See figure 9. Trim by stern shows clearly less influence of the cross flow which is even almost negligible for both forward sections. For the largest draught it appears that the cross flow is dominant for the aft part of the model while speed influence is clearly shown at the sections 3 and 4. The smallest draught condition demonstrates little influence of cross flow for the lowest speed and only for the aft part of the model for drift angles above 12 degrees. For the highest speed the variation is remarkable for the sections 4, 5 and 6 while the influence for section 7 may be neglected. The longitudinal distribution of the total drift force coefficient generally shows little influence of the drift angle. See figure 6 and 7. The value for the foremost segment is most significant with respect to the even keel conditions and the bow trim condition. For trim by stern all sections experience an almost equal contribution with increased values in negative direction. For the largest draught both forward sections show a strong increase of the total drift force while the contributions from after the second section are very small. There is also a slight increase of the total drift force in the positive direction for the midship section. Strong reduction of the total drift force is shown for the small draught with almost no contribution after the midship section.

#### CONCLUSIONS AND RECOMMENDATIONS

The following conclusions and recommendations may be derived from this study:

1. In general the experiments indicate that there is little forward speed influence on the drift force components.
2. Related to drift angle it appeared that the coefficients increase almost linearly with this angle except the linear drift force component which by definition remains independent on drift angle. Cross flow may be neglected below a drift angle of about 4 degrees.
3. The total drift force coefficient and the components increase with draught and trim by stern with an exception for the cross flow producing higher values at bow trim.
4. For more shallow water ( $h/T = 2.4$ ) combined with lower speeds the cross flow drag coefficient decreases considerably.

5. With respect to the longitudinal distribu-  
tion of the drift force coefficients it has  
been shown that forward sections provide a  
dominant part of the drift forces except in  
case of trim by stern when higher negative  
drift force coefficients arise with a more  
equal longitudinal distribution. For cross  
flow there is an increase on the aft part  
of the model at larger draughts and bow  
trim. Speed influence by wave generation is  
shown locally at the forward sections.
6. The calculated distribution of the linear  
drift force coefficient shows a rather good  
agreement with the experimental results for  
the forward part of the model. Integration  
over 60 percent of the forward length of  
this distribution curve provides useful re-  
sults for the linear drift force and moment  
in case of even keel condition in both deep  
and shallow water. The shallow water influ-  
ence becomes already significant at a water  
depth draught ratio  $h/T=5$ .
7. More investigations should be carried out  
to determine which accuracy of the hydrody-  
namic derivatives is required to admit a  
certain deviation in the manoeuvring track  
to be predicted.
8. Especially at the ends the distribution of  
the drift forces remains doubtful. For a  
better estimation it is recommended to use  
a row of pressure transducers in longitudi-  
nal direction at the ends.
9. In order to investigate flow separation  
phenomena, more extensive research should  
be performed especially at the aft part of  
the model.

#### REFERENCES

- [1] Hoofft, J.P., Discussion MN-3, 18th ITTC,  
volume 2, 1988, Kobe Japan, pp. 181-191.
- [2] Clarke, D., A two-dimensional strip method  
for surface ship hull derivatives: Compar-  
ison of theory with experiments on a  
segmented model, Journal of Mechanical  
Engineering Science, Vol.14, Nr.7, 1972.
- [3] Burcher, R.K., Developments in ship ma-  
noeuvrability, Transactions RINA, volume  
114, 1972.
- [4] Matsumoto, Norihiro and Suemitsu Keyi,  
Hydrodynamic force acting on a hull in  
manoeuvring motion, Journal of the Kansai  
Soc. of Naval Arch., Japan, No.190, 1983
- [5] Beukelman, W. and Gerritsma, J., The long-  
itudinal distribution of low frequency  
hydrodynamic derivatives for lateral mo-  
tions in shallow water, Ship Hydrome-  
chanics Laboratory, Delft University of  
Technology, Report No.562A, September '83
- [6] Beukelman, W., On sway damping and added  
mass in shallow water, 17th ITTC, Volume  
2, 1984, Goteburg Sweden, pp. 188
- [7] Hirano Masayoshi, Takashina Junshi,  
Moriya Shuko and Nakamura Yoshiaki, An  
experimental study on manoeuvring hydro-  
dynamic forces in shallow water, Trans-  
actions of the West-Japan Society of  
Naval Architects, No.69, March 1985.

- [8] Inoue Shosuke, Kyima Katsuro and Moriyama  
Fumio, Presumption of hydrodynamic deri-  
vatives on ship manoeuvring in trimmed  
condition, Transactions of the West-Japan  
Society of Naval Architects, No.55, 1978
- [9] Inoue Shosuke, Hirano Masayoshi and Kyima  
Katsuro, Hydrodynamic derivatives on ship  
manoeuvring, International Shipbuilding  
Progress, Vol.28, No.321, May 1981.
- [10] Gerritsma, J., Hydrodynamic derivatives  
as a function of draught and ship speed,  
Ship Hydromechanics Laboratory, Delft  
University of Technology, Report No.477,  
January 1979.
- [11] Beukelman, W., Longitudinal distribution  
of drift forces for a ship model, Ship  
Hydromechanics Laboratory, Delft Univer-  
sity of Technology, Report No.810, Decem-  
ber 1988.
- [12] Keil, H., Die hydrodynamische kräfte bei  
der periodischen Bewegung zweidimensiona-  
ler Körper an der Oberfläche flacher ge-  
wasser, Institut für Schiffbau der Uni-  
versität Hamburg, Bericht no.305, Februar  
1974.
- [13] Norrbin, N.H., Theory and observations on  
the use of a mathematical model for ship  
manoeuvring in deep and confined waters,  
The Swedish State Shipbuilding Experimen-  
tal Tank, Goteburg Sweden, Publication 68  
1971.
- [14] Inoue Shosuke, The determination of trans-  
verse hydrodynamic non-linear forces by  
means of steady turning, 11th ITTC, Tokyo,  
1966, pp.542.

Table 3a

Sect. nr.	$y_{\dot{y}}^n * 10^3 - - m' / (4\rho L^3) * 10^3$						
	$h/T=$ 5.000	$h/T=$ 7.7	$h/T=$ 15	$h/T=$ 5	$h/T=$ 2.4	$h/T=$ 1.5	$h/T=$ 1.15
0	-0.0	-0.2	-0.2	-0.2	-0.2	-0.2	-0.3
1	-3.7	-3.7	-3.7	-3.8	-4.1	-5.0	-7.6
2	-3.6	-3.6	-3.6	-3.7	-4.2	-5.8	-10.2
3	-3.9	-3.9	-3.9	-4.1	-4.9	-7.6	-15.6
4	-4.3	-4.3	-4.4	-4.6	-5.9	-9.9	-22.2
5	-4.9	-4.9	-4.9	-5.3	-7.1	-12.5	-29.2
6	-5.5	-5.5	-5.5	-6.0	-8.2	-15.0	-37.6
7	-5.9	-6.0	-6.0	-6.6	-9.0	-16.8	-44.0
8	-6.2	-6.2	-6.3	-6.8	-9.4	-17.8	-46.3
9	-6.3	-6.3	-6.4	-6.9	-9.6	-18.1	-46.3
10	-6.3	-6.3	-6.4	-6.9	-9.6	-18.1	-46.3
11	-6.3	-6.3	-6.4	-6.9	-9.6	-18.1	-46.3
12	-6.3	-6.3	-6.4	-6.9	-9.6	-18.1	-46.3
13	-6.1	-6.1	-6.2	-6.8	-9.3	-17.5	-48.1
14	-5.9	-5.9	-5.9	-6.5	-8.8	-16.5	-42.7
15	-5.5	-5.5	-5.5	-6.0	-8.0	-14.5	-36.3
16	-5.2	-5.2	-5.2	-5.6	-7.2	-12.4	-29.8
17	-4.8	-4.8	-4.9	-5.1	-6.3	-10.1	-22.8
18	-4.6	-4.6	-4.7	-4.8	-5.6	-8.2	-16.5
19	-4.5	-4.5	-4.5	-4.6	-5.1	-6.6	-11.2
20	0	0	0	0	0	0	0

Table 3b

Sect. nr.	$Y_V^h * 10^3 - U \frac{dm^i}{dx} * 10^3 / (h\rho L^2 U)$						
	$h/T=5000$	$h/T=77$	$h/T=15$	$h/T=5$	$h/T=2.4$	$h/T=1.5$	$h/T=1.15$
0	71.2	71.2	71.4	72.9	79.0	97.9	146.3
1	34.0	34.0	34.1	35.4	40.6	56.2	99.6
2	1.3	1.3	1.5	2.7	8.2	25.7	80.3
3	7.5	7.5	7.8	9.5	17.1	41.7	119.9
4	10.6	10.6	10.8	12.8	21.6	50.1	143.1
5	11.9	12.0	12.1	14.2	22.9	52.1	153.7
6	10.6	10.6	10.8	12.4	19.5	43.9	141.4
7	7.2	7.2	7.2	8.3	12.8	28.3	87.8
8	3.4	3.4	3.4	3.9	6.0	12.9	22.9
9	0.9	0.9	0.9	1.0	1.6	3.4	0
10	0	0	0	0	0	0	0
11	0	0	0	0	0	0	0
12	-1.6	-1.6	-1.6	-1.8	-2.7	-6.0	29.0
13	-4.1	-4.1	-4.1	-4.8	-7.5	-16.9	-36.3
14	-6.5	-6.5	-6.7	-7.8	-13.0	-30.5	-117.7
15	-7.3	-7.3	-7.5	-9.2	-16.6	-40.9	-129.2
16	-6.7	-6.7	-6.9	-8.8	-17.4	-44.9	-135.5
17	-5.2	-5.2	-5.4	-7.4	-15.9	-43.6	-133.2
18	-3.4	-3.4	-3.6	-5.2	-12.4	-36.4	-115.7
19	-47.3	-47.3	-47.5	-49.3	-57.4	-82.9	-164.7
20	-91.4	-91.4	-91.8	-94.0	-103.7	-133.4	-223.6

Table 4

h/T	CALCULATION (KEIL)			EXPERIMENT			CALCULATION		
	$m' \text{ -ord.8}$ kg/m	$Y_V^h * 10^3 - \frac{m'}{h\rho L} * 10^3$	$N_V^h * 10^3 - \int_{ord.8}^{pp} Y_V^h dx$	$Y_V^h * 10^3$	$N_V^h * 10^3$	$F_n$	$Y_V^h * 10^3$	$N_V^h * 10^3$	METHOD
$\infty$	37.4	-14.2	-5.7				-17.2	-6.4	NORRBIN
$\infty$							-15.0	-6.6	INOUE
77	37.4	-14.2	-5.7						
15	37.4	-14.2	-5.7	-14.8	-5.8	0.15			
				-15.0	-5.9	0.20			
				-16.1	-6.7	0.25			
5	41.4	-15.7	-6.2						
2.4	56.9	-21.6	-8.2	-21.6	-7.1	0.0675			
				-19.6	-7.4	0.103			
				-36.5	-12.2	0.0675			
1.5	107.5	-40.9	-14.4	-32.7	-12.0	0.103			
				-145.3	-27.2	0.0675			
				-113.8	-24.1	0.103			

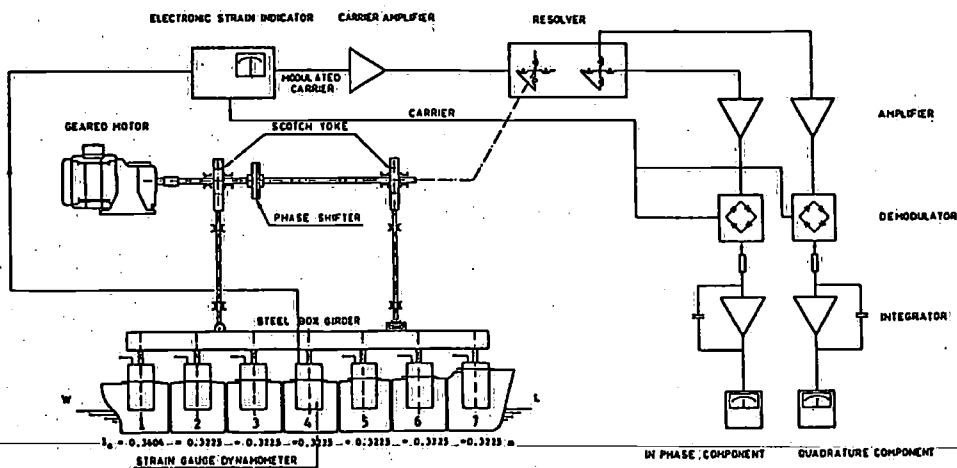


Figure 1. Principle of mechanical oscillator and electronic circuit.

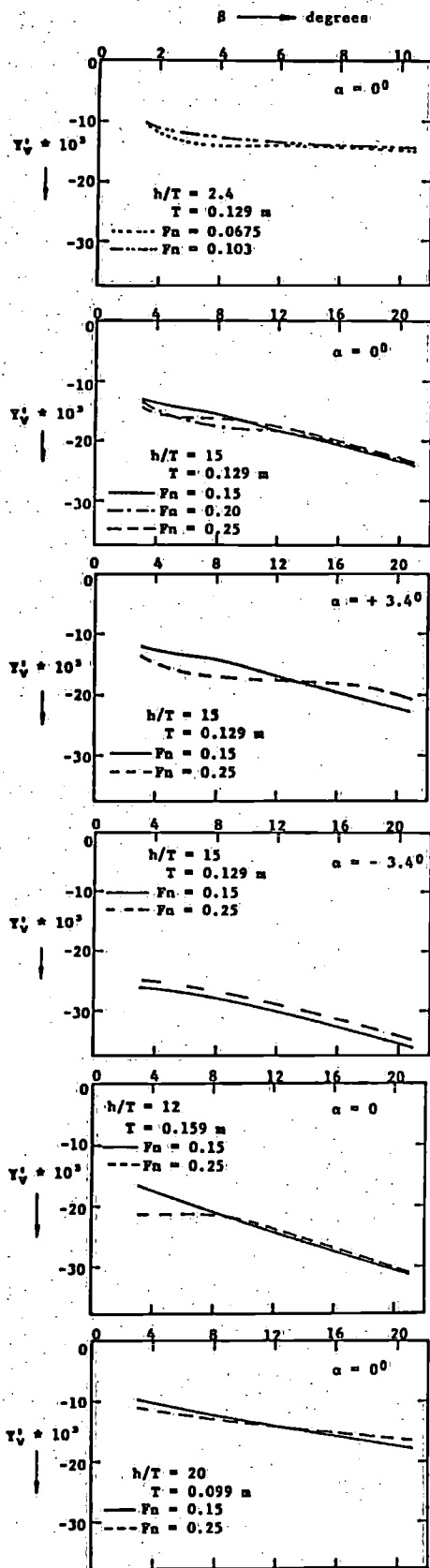


Figure 2. Total measured non-dimensional drift force  $Y_V$  for the whole model related to drift angle.

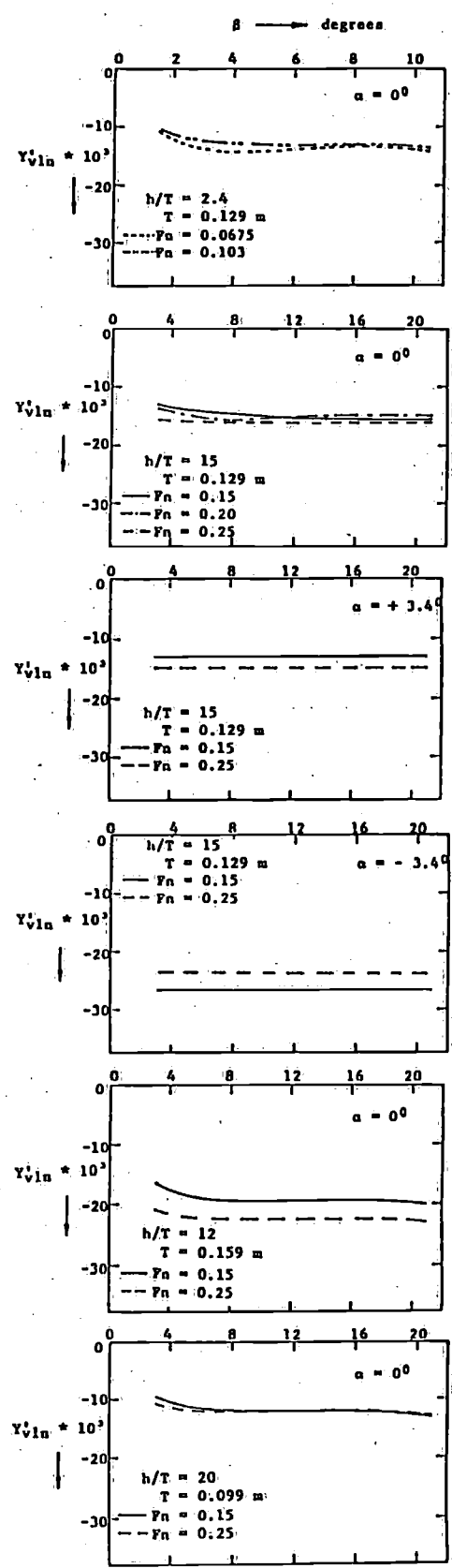


Figure 3. Non-dimensional linear drift force  $Y_{Vlin}$  for the whole model related to drift angle.



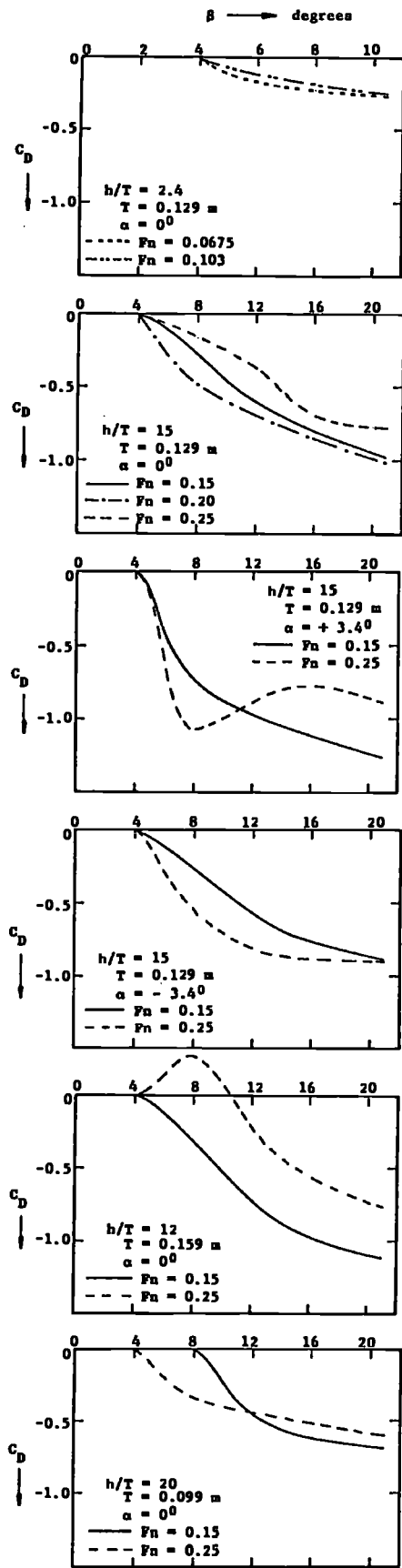


Figure 4. Cross flow drag coefficient for the whole model related to drift angle.

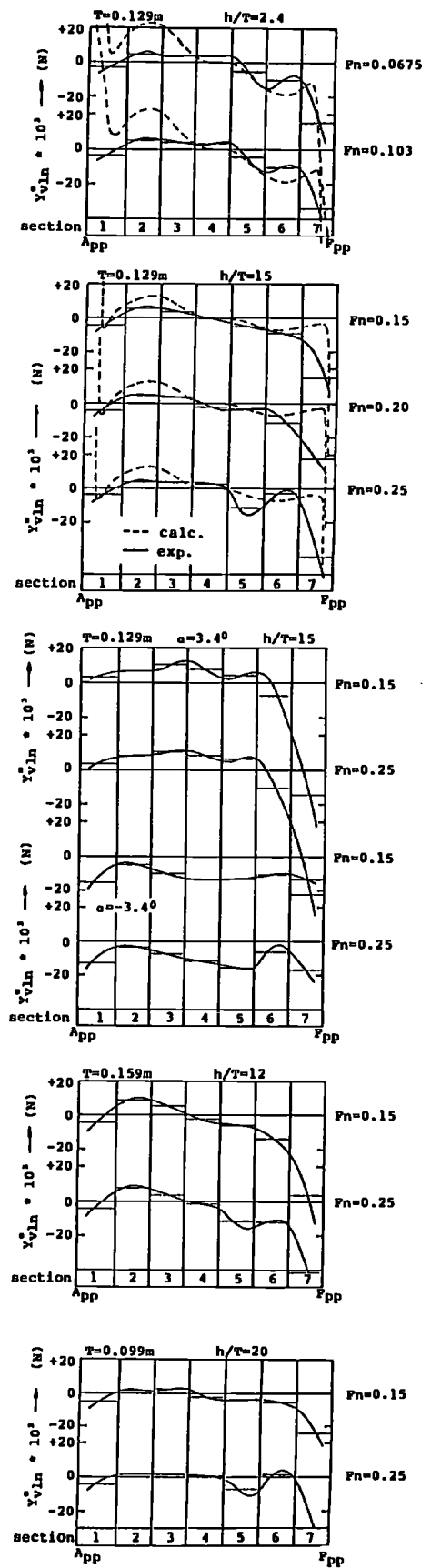


Figure 5. Longitudinal distribution of the non dimensional linear drift force  $Y_{vln}$ .

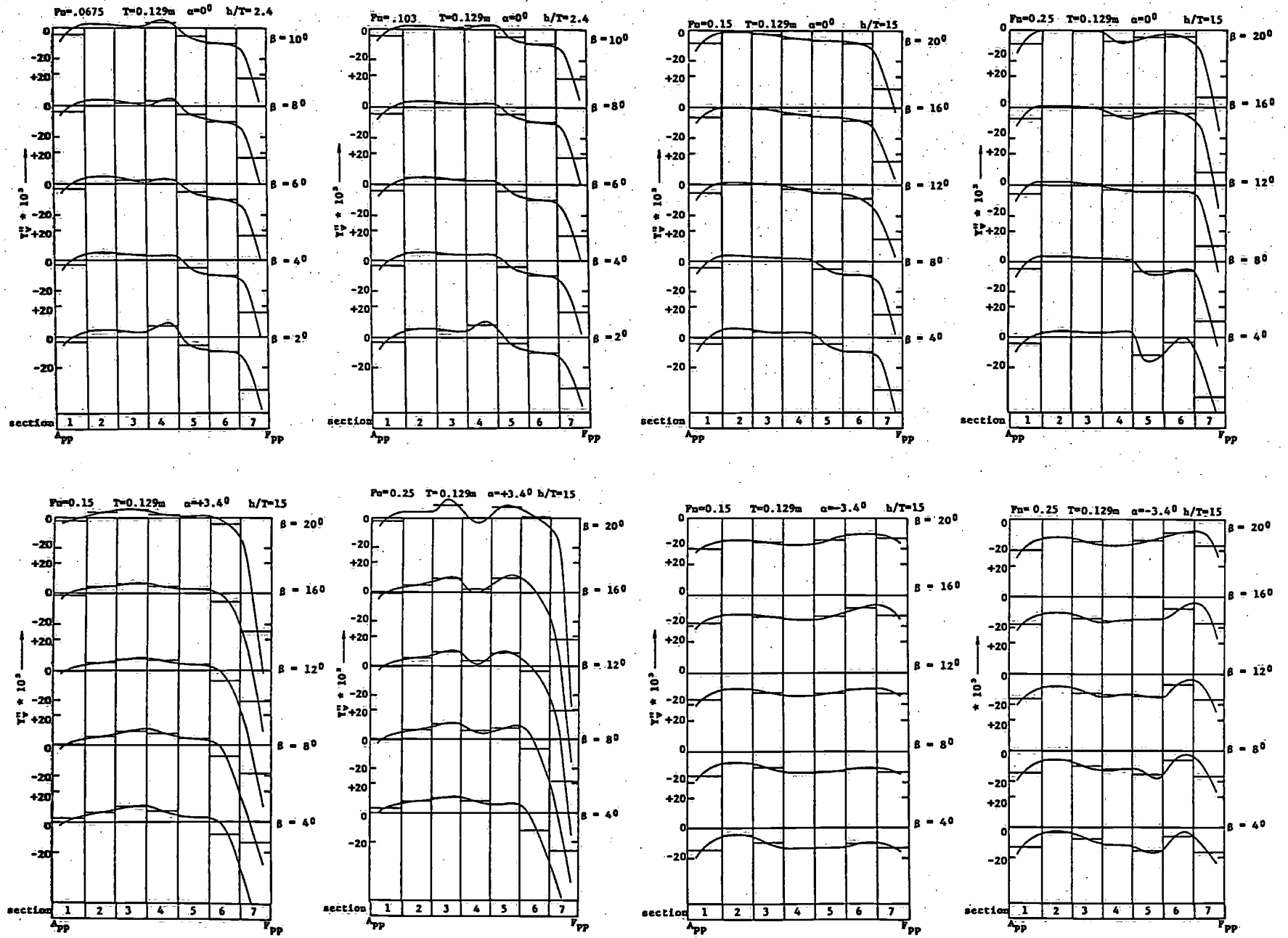


Figure 6. Longitudinal distribution of the total measured non-dimensional drift force  $Y_v^m$ .

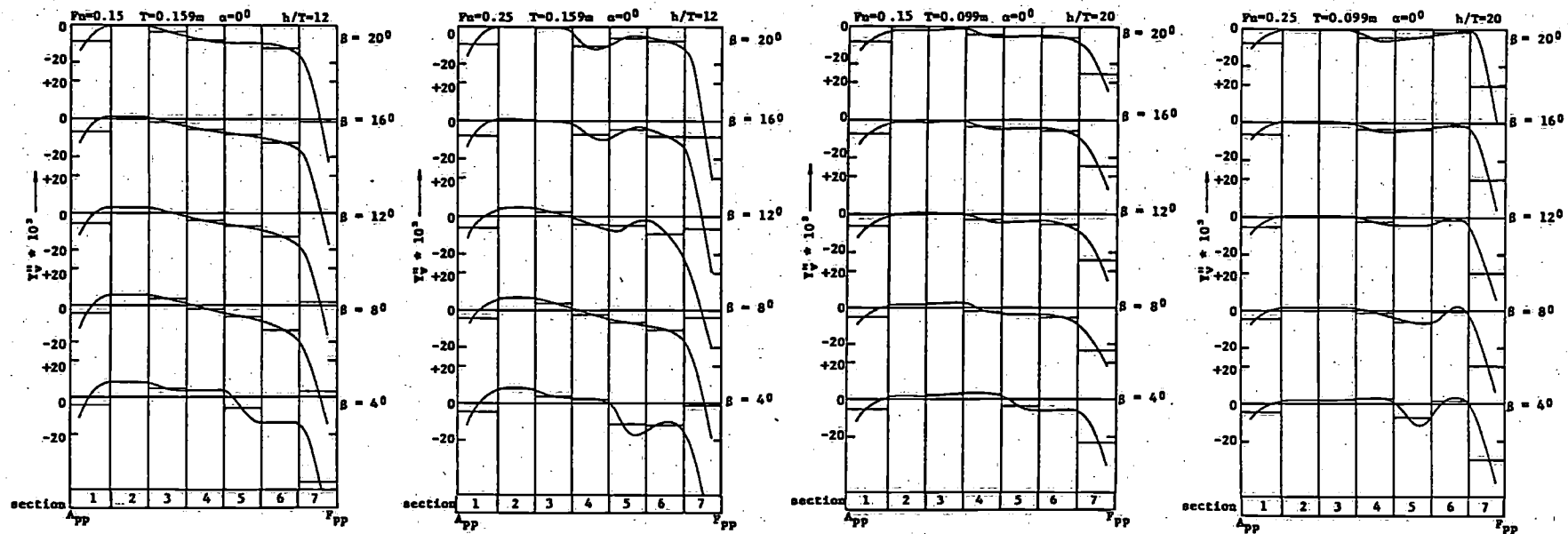


Figure 7. Longitudinal distribution of the total measured non-dimensional drift force  $Y_v^n$ .

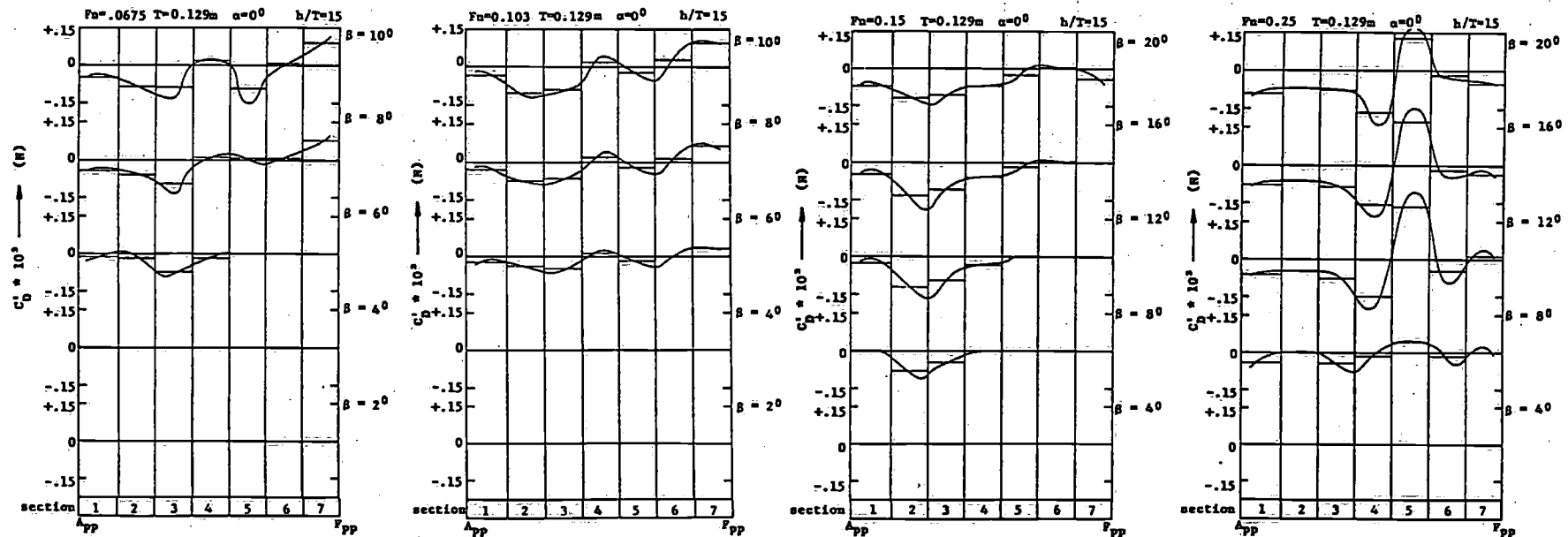


Figure 8. Longitudinal distribution of the cross flow drag coefficient  $C_D$ .

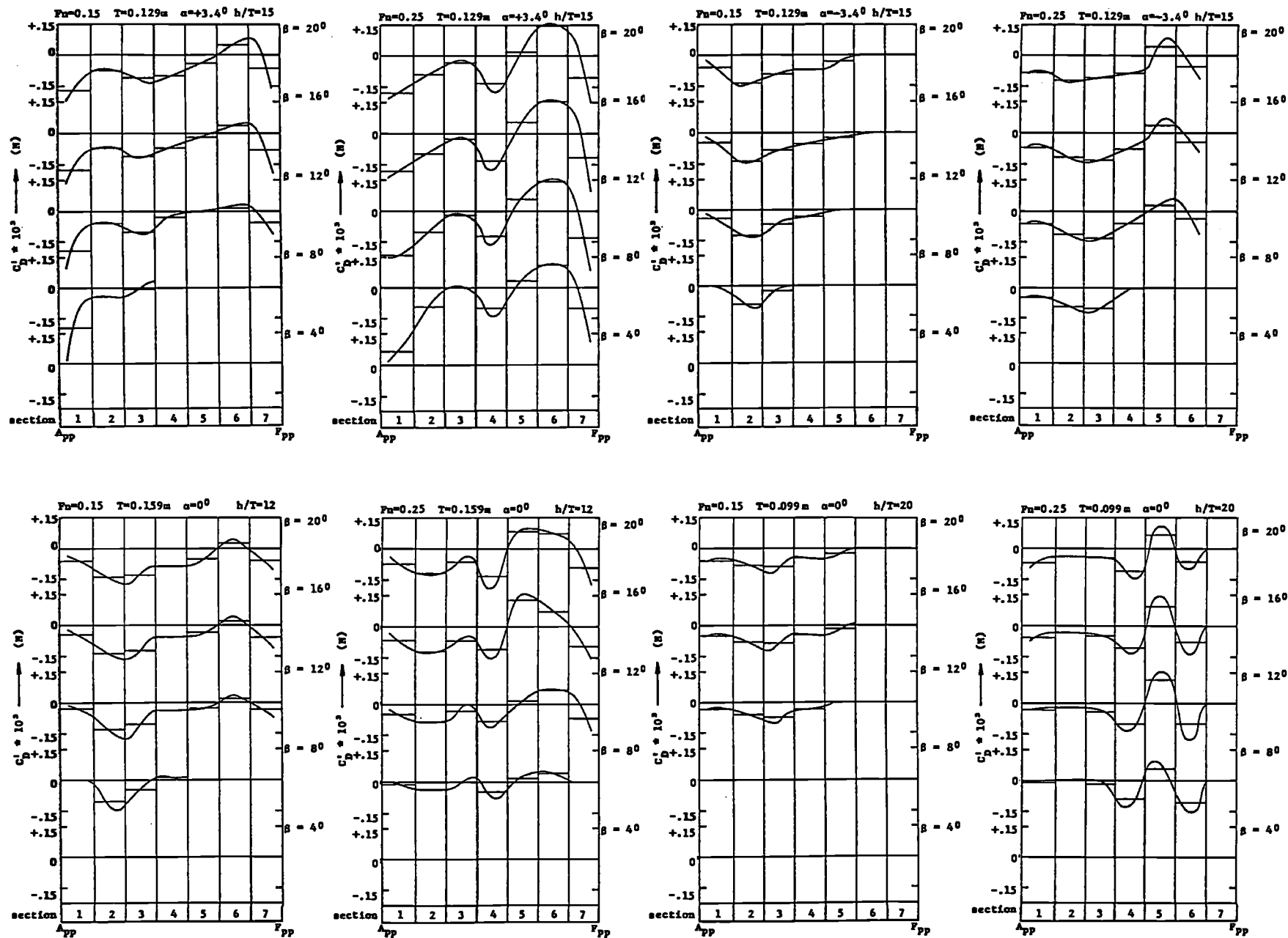


Figure 9. Longitudinal distribution of the cross flow drag coefficient  $C_D$ .